

Effect of viscosity contrast on vesicle dynamics in linear flows

Petia M. Vlahovska* and Ruben Serral Gracia

Max-Planck Institute of Colloids and Interfaces, Potsdam-Golm, Germany

(Dated: December 2, 2024)

Abstract

We develop a small-deformation theory for the dynamics of a quasi-spherical vesicle in viscous flows. The analysis takes into account the membrane incompressibility and includes the viscosity contrast between the inner and suspending fluids and the membrane bending stresses. The leading order shape evolution equation is derived. The analytical results show that the stationary vesicle shape and orientation angle with respect to the flow are independent of the membrane bending rigidity. Non-Newtonian rheology with both shear thinning viscosity and normal stresses is predicted for a dilute suspension of vesicles. In the tumbling regime, the vesicle exhibits periodic shape deformations with a frequency that increases with the viscosity contrast. The theory is in good agreement with published experimental data for vesicle behavior in simple shear flow.

PACS numbers: 47.15.G-, 83.50.-v, 87.16Dg

I. INTRODUCTION

Dynamics of deformable particles such as drops, capsules and cells in flow represents a long-standing problem of interest because of its relevance to rheology of emulsions and biological suspensions such as blood. The problem is challenging because the shape of these “soft” particles is not given *a priori* but is governed by the balance between interfacial forces, e.g. due to stretching and/or bending of the interface, and fluid stresses. The interfacial properties, therefore, play a crucial role in the dynamics of these particles.

Microhydrodynamics of drops and capsules has been studied extensively^{1,2,3}. The drop interface is governed by tension, which in the absence of surfactants is isotropic; surfactants can give rise non-uniform tension and shear and dilatational viscous stresses. Capsule membranes are made of polymeric materials, which, in addition to the above mentioned stresses, can generate interfacial stresses of a more complicated nature, e.g. neo-Hookean. Typically, drops and capsules have no bending resistance and their interface is compressible, i.e the total area can vary when subjected to an external flow. For example, a drop in shear flow deforms into an ellipsoid. As the flow strength increases, the drop area also increases and the angle between the ellipsoid major axis and flow direction decreases from $\pi/4$. If flow strength is sufficiently high the drop breaks up.

Vesicles formed by a closed lipid bilayer membrane are widely employed as a cell paradigm⁴. The nature of the bilayer introduces two new features in the problem: bending rigidity and membrane incompressibility. Equilibrium mechanical properties of vesicles made of artificial membranes are fairly well understood⁵. Vesicles exhibit a variety of equilibrium shapes that correspond to minima of the membrane bending energy for a given volume-to-area ratio⁵. Experimental studies^{6,7,8,9} of vesicle behavior in unbounded shear flow observe that in weak flows and when the inner and outer fluids are the same the vesicle deforms into a tank-treading stationary prolate ellipsoid with inclination angle with respect to the flow direction close to $\pi/4$; however, in striking contrast to drops, when the fluid inside is more viscous than the outside the vesicle undergoes a tumbling motion.

Numerical simulations^{10,11,12} and analytical theories^{13,14,15} of vesicle microhydrodynamics that attempt to elucidate the experimental observations are limited. In their classic paper Keller and Skalak¹⁶ analyzed the motion of a tank-treading ellipsoid in shear flow. The theory qualitatively captures features like the tumbling transition but the assumptions of

a fixed particle shape questions the model applicability to deformable vesicles. The free-boundary character of the problem is taken into account in several recent works. Shape evolution of a fluctuating quasi-spherical vesicle was considered by Seifert¹³ for the case when the inner and suspending fluids are the same, i.e. there is no viscosity contrast. The theory predicts a stationary, tank-treading prolate ellipsoid and no transition to tumbling motion. The importance of viscosity contrast for the tumbling transition was recognized by Misbah¹⁴, who showed quantitatively that the critical value of viscosity contrast decreases with the volume-to-surface ratio. He also pointed out that the area constraint leads to non-linear leading order evolution equations for the vesicle shape, which in the case when only ellipsoidal deformation modes are considered are independent of the membrane bending rigidity. Similar results were derived by Olla¹⁵ whose analysis was based on a different approach to describe membrane stresses that considers a membrane of non-zero thickness.

Another interesting aspect of the vesicle microhydrodynamics is the vesicle behavior near a wall. Flow-induced deformation of an adhering vesicle gives rise to a lift force that can lead to unbinding from the substrate^{17,18,19}. The experiments have not been yet quantitatively compared to theoretical studies^{20,21,22}.

The purpose of this paper is to include the effects of viscosity contrast and membrane bending rigidity in the analysis of vesicle dynamics in shear flows and to provide a quantitative description of the experimentally observed vesicle behavior. As a first step, the leading order small deformation of a quasi-spherical vesicle will be considered. However, the developed formalism will serve as a rigorous basis for considering higher orders in the non-linear dynamics of a vesicle in flow.

II. PROBLEM FORMULATION

Let us consider a neutrally-buoyant vesicle suspended in an incompressible fluid of viscosity η . The vesicle is filled with an incompressible fluid of viscosity $(\lambda - 1)\eta$ bound by an inextensible membrane of zero thickness characterized by fixed area A and bending rigidity modulus κ . The vesicle has a characteristic size a defined by the radius of a sphere of the same volume. The equilibrium shape of the vesicle is characterized by a small excess area

$$\Delta = A/a^2 - 4\pi. \quad (1)$$

A. Governing equations

The vesicle is placed in a steady two-dimensional linear flow

$$\mathbf{v}^\infty(\mathbf{r}) = \dot{\gamma} \mathbf{E} \cdot \mathbf{r}, \quad (2)$$

where $\dot{\gamma}$ is the strain rate, and \mathbf{E} is the velocity gradient. Linear flows are defined by

$$\mathbf{E} = \frac{1}{2} \begin{pmatrix} 0 & 1 + \omega & 0 \\ 1 - \omega & 0 & 0 \\ 0 & 0 & 0 \end{pmatrix}, \quad (3)$$

where ω is the magnitude of the rotational flow component. Irrotational flows such as straining flow are given by $\omega = 0$. Simple shear flow is specified by $\omega = 1$.

Typically vesicles are micron-sized. At these length-scales water is effectively very viscous, inertial effects are unimportant and fluid velocity fields inside \mathbf{v}^{in} and outside \mathbf{v}^{out} the vesicle are described by the Stokes equations

$$\begin{aligned} \eta \nabla^2 \mathbf{v}^{\text{out}} - \nabla p^{\text{out}} &= 0, & \nabla \cdot \mathbf{v}^{\text{out}} &= 0, \\ (\lambda - 1) \eta \nabla^2 \mathbf{v}^{\text{in}} - \nabla p^{\text{in}} &= 0, & \nabla \cdot \mathbf{v}^{\text{in}} &= 0. \end{aligned} \quad (4)$$

Far away from the vesicle, the flow field tends to the unperturbed external flow $\mathbf{v}^{\text{out}} \rightarrow \mathbf{v}^\infty$. Velocity is continuous across the membrane

$$\mathbf{v}^{\text{in}} = \mathbf{v}^{\text{out}} \equiv \mathbf{v}_s \quad \text{at } r = r_s. \quad (5)$$

The membrane moves with the fluid velocity $\mathbf{v}_s \cdot \mathbf{n}$, where \mathbf{n} is the outward pointing unit normal vector to the interface. Shape evolution is discussed in Appendix B. Fluid motion exerts viscous stresses on the membrane that are balanced by membrane stresses due to the nonequilibrium membrane configuration

$$\mathbf{t} = 2\sigma H \mathbf{n} - \kappa [4H^3 - 4KH + 2\nabla_s^2 H] \mathbf{n} - \nabla_s \sigma. \quad (6)$$

Here H and K are the mean and Gaussian curvatures, respectively, and σ is the local membrane tension. The surface gradient operator is defined as

$$\nabla_s = \mathbf{I}_s \cdot \nabla, \quad (7)$$

where $\mathbf{I}_s = \mathbf{I} - \mathbf{n}\mathbf{n}$ represents surface projection.

Since the number of lipids in the membrane and the area per lipid are fixed, the total vesicle area is constant and the membrane behaves as an incompressible material, i.e. a membrane element only deforms but does not change its area. The local area conservation $DA/Dt = 0$ implies that the velocity field at the interface is irrotational¹³

$$\nabla_s \cdot \mathbf{v} = 0 \quad (8)$$

Accordingly, the local tension σ changes in order to keep the local area constant. The membrane incompressibility is analogous to the fluid incompressibility, where finite changes in pressure correspond to infinitesimal changes in fluid density, and pressure takes the place of the density as an independent field variable. In that respect, parallels can be drawn between vesicles and spherical drops covered with an incompressible surfactant film²³.

B. Dimensionless parameters

In the case of drops, deformation is inhibited by strong surface tension or when the internal fluid is more viscous than the outer fluid and the vorticity is non-zero². Similar conclusions can be drawn for vesicles.

Shape deformation by the viscous forces exerted by the extensional component of the external flow occurs on the time scale

$$t_{\dot{\gamma}} = \lambda \dot{\gamma}^{-1}, \quad (9)$$

where $\lambda = \eta^{\text{in}}/\eta^{\text{out}} + 1$. Several mechanisms control the magnitude of shape distortion. Bending stresses work to bring the shape back to its preferred curvature state; the corresponding time scale is

$$t_{\kappa} = \frac{\lambda \eta a^3}{\kappa}. \quad (10)$$

In shear flow, vesicle rotation away from the extensional axis of the imposed flow effectively decreases the extent of shape distortion; the associated time scale is

$$t_r = \dot{\gamma}^{-1}. \quad (11)$$

The strength of these two relaxation mechanisms that limit shape deformation by the flow is quantified by the corresponding dimensionless parameters: the capillary number

$$\chi = \frac{t_{\kappa}}{t_{\dot{\gamma}}}, \quad (12)$$

and the rotation parameter

$$R = \frac{t_r}{t_{\dot{\gamma}}} = \lambda^{-1}. \quad (13)$$

The smaller of these parameters controls the magnitude of vesicle deformation. At moderate viscosity ratios, the vesicle shape remains close to the equilibrium one provided that the capillary number is small, i.e. the flow is weak. High viscosity inner fluid limits the shape distortion by means of increasing the rate of vesicle rotation. In addition to the flow-related parameters, a physical parameter that arises from vesicle geometry is the excess area (1) which sets the maximum magnitude of the shape distortion.

Henceforth, bending stresses and tension are normalized by κ/a^2 ; all other quantities are rescaled using η , a , and $\dot{\gamma}$. Accordingly, the time scale is $\dot{\gamma}^{-1}$, the velocity scale is $\dot{\gamma}a$, bulk stresses are scaled with $\eta\dot{\gamma}$.

III. SMALL DEFORMATION THEORY

In this section we present a perturbative solution for the micro-hydrodynamics of a vesicle with shape close to a sphere.

In a coordinate system centered at the vesicle, the radial position r_s of the vesicle interface can be represented as

$$r_s = \alpha + f(\Omega), \quad (14)$$

where Ω is the solid angle and f is the deviation of vesicle shape from a sphere, which depends only on the angle Ω and has a vanishing angular average

$$\int f \, d\Omega = 0. \quad (15)$$

The isotropic contribution α is determined by the volume-conservation constraint

$$\int (\alpha + f)^3 \, d\Omega = 4\pi. \quad (16)$$

The total area conservation constraint relates the amplitude of the perturbation f and the excess area Δ

$$\int \frac{r_s^2}{\hat{\mathbf{r}} \cdot \mathbf{n}} \, d\Omega = 4\pi (1 + \Delta). \quad (17)$$

where $\hat{\mathbf{r}}$ denotes the unit radial vector.

A. Expansion in spherical harmonics

In Eq. (14), the function f representing the perturbations of the vesicle shape depends only on angular coordinates. Thus, it is expanded into series of scalar spherical harmonics Y_{jm} (A1)

$$f = \sum_{j=2}^{\infty} \sum_{m=-j}^j f_{jm} Y_{jm}, \quad (18)$$

In the above equation, the summation starts from nonzero j because f includes only the nonisotropic contributions.

Likewise, the nonuniform tension is expanded in scalar spherical harmonics

$$\sigma = \sigma_0 + \sum_{j=2}^{\infty} \sum_{m=-j}^j \sigma_{jm} Y_{jm}, \quad (19)$$

where σ_0 is the isotropic part of the tension, which varies with shape in order to keep the total area constant as discussed in details in Appendix D.

Velocity fields are described using basis sets of fundamental solutions of the Stokes equations²⁴, \mathbf{u}_{jmq}^{\pm} , defined in Appendix E:

$$\begin{aligned} \mathbf{v}^{\text{out}}(\mathbf{r}) &= \sum_{jmq} c_{jmq}^{\infty} [\mathbf{u}_{jmq}^+(\mathbf{r}) - \mathbf{u}_{jmq}^-(\mathbf{r})] \\ &+ \sum_{jmq} c_{jmq} \mathbf{u}_{jmq}^-(\mathbf{r}), \end{aligned} \quad (20a)$$

$$\mathbf{v}^{\text{in}}(\mathbf{r}) = \sum_{jmq} c_{jmq} \mathbf{u}_{jmq}^+(\mathbf{r}). \quad (20b)$$

For small shape perturbations around a sphere the volume constraint (16) becomes^{13,25}

$$\alpha = 1 - \frac{1}{4\pi} \sum_{jm} f_{jm} f_{jm}^* + O(f^3), \quad (21)$$

where the sum over j starts from 2, $|m| < j$ and $f_{jm}^* = (-1)^m f_{j-m}$. Similarly, the area constraint (17) transforms to

$$\Delta = \sum_{jm} a(j) f_{jm} f_{jm}^* + O(f^3), \quad (22a)$$

where

$$a(j) = \frac{(j+2)(j-1)}{2}. \quad (22b)$$

B. Perturbation solution

The combination of perturbative analysis and spherical harmonics formalism for solving Stokes-flow problems involving a deformable particle has been developed in details in Vlahovska *et al.*^{25,26} on the example of a surfactant-covered drop. Here we present a brief outline of the method, and focus on the new features specific to membranes such as the area constraint and tension.

This paper focuses on a quasi-spherical vesicle, with the magnitude of the shape deviation from sphericity given by ε , i.e. $f \sim O(\varepsilon)$. For small perturbations, $\varepsilon \ll 1$, the exact position of the interface at $r = 1 + \varepsilon \tilde{f}$ is replaced by the equilibrium position, $r = 1$, and all quantities that are to be evaluated at the interface of the deformed drop are approximated using a Taylor series expansion. In the case of vesicles, the small parameter is set by the geometrical constraint for constant total area (22)

$$\varepsilon = \Delta^{\frac{1}{2}}. \quad (23)$$

The leading order solution is presented in details in Appendix C. The resulting shape evolution equation (B8) is

$$\dot{f}_{jm} = \omega \frac{im}{2} f_{jm} + \lambda^{-1} C(\lambda, j, m) + \lambda^{-1} \chi^{-1} \Gamma(\lambda, \sigma_0, j) f_{jm} + O(\lambda^{-1} \varepsilon, \varepsilon^2), \quad (24)$$

where the tension σ_0 is determined using the area constraint (22) as described in Appendix D, see Eq. (D5). The first term in the evolution equation (24) describes rigid body rotation of a particle with shape f by the rotational component of the external flow. The second term describes the distortion of the vesicle shape by the extensional component of the external flow. The term including χ is associated with relaxation driven by interfacial stresses. The expressions for C and Γ are given by (C9). These coefficients depend on λ and are bounded at $\lambda \rightarrow \infty$.

The area constraint couples all modes thereby making the leading order vesicle dynamics non-linear. As we show in the next section, an interesting consequence of the constrained dynamics is that the stationary solution is independent of the membrane properties (even though the transient period of the approach to steady state is affected by the bending stiffness). In addition, if the extensional component of the external flow perturbs only

modes with a certain \hat{j} , e.g. in shear flow $\hat{j} = 2$, all modes with $j \neq \hat{j}$ decay and the dynamics at long times becomes independent of the membrane bending rigidity.

IV. RESULTS: SIMPLE SHEAR FLOW

In this section we provide analytical solutions for the vesicle shape evolution in a simple shear flow (2), which in the spherical harmonics representation (20) is specified by an extensional component

$$c_{2\pm 20}^{\infty} = \mp i\sqrt{\frac{\pi}{5}} \quad c_{2\pm 22}^{\infty} = \mp i\sqrt{\frac{2\pi}{15}}, \quad (25a)$$

and a rotational component

$$c_{101}^{\infty} = i\sqrt{\frac{2\pi}{3}}. \quad (25b)$$

The extensional part of external flow (2), which is responsible for shape distortion, is fully characterized by a second-order traceless tensor, which corresponds to spherical harmonics of the order $j = 2$ (25a). Therefore, at leading order the shear flow affects only the subspace $j = 2$. Considering only these modes simplifies the expression for the tension (D5) and the evolution equations (24) to the following set of coupled non-linear differential equations

$$\begin{aligned} \dot{f}_{2m} = & -\frac{im}{2}h(\lambda)\delta_{|m|2} + \frac{im}{2}f_{2m} \\ & - 2ih(\lambda)\Delta^{-1}(f_{22} - f_{2-2})f_{2-m} \end{aligned} \quad (26)$$

where

$$h(\lambda) = \frac{4\sqrt{30\pi}}{23\lambda + 9}. \quad (27)$$

Strictly speaking Eq. (26) is only valid at long times ($t \gg \chi$) when all $j \neq 2$ modes have decayed. The initial conditions are set by the equilibrium vesicle configuration. For example, for a fluctuating quasi-spherical vesicle¹³

$$|f_{jm}|^2 = \frac{k_B T}{\kappa E(j, \sigma_{\text{eq}})}, \quad (28)$$

where $E(j, \sigma)$ is given by (C9d).

The shape parameters (18) are decomposed into real and imaginary parts

$$f_{jm} = f'_{jm} + if''_{jm} \quad f_{jm}^* = f'_{jm} - if''_{jm} \quad (29)$$

In the flow plane $x - y$, vesicle shape f is characterized by only three components, f'_{22} , f''_{22} , and f_{20} , corresponding to deformation along the flow axis x , straining axis $x = y$, and the z axis. Shape modes $f_{2\pm 1}$ describe deformations of the type xz and yz , which vanish in the flow plane $z = 0$. From geometrical considerations we have for the inclination angle

$$\phi_0 = -\frac{1}{2} \arctan \left(\frac{f''_{22}}{f'_{22}} \right). \quad (30)$$

A. Tank-treading

The evolution equations (26) have two sets of stationary points. The first one corresponds to the tank-treading state. The only non-zero stationary amplitudes are

$$f''_{22} = -\frac{\Delta}{4h(\lambda)} \sqrt{-1 + \frac{4h^2(\lambda)}{\Delta}}, \quad f'_{22} = \frac{\Delta}{4h(\lambda)}. \quad (31)$$

The numerical solution of the full set of evolution equations (24) shows that all other modes decay to zero. Hence, in the stationary state all excess area is stored in the $f_{2\pm 2}$ modes. Substituting the stationary amplitudes (31) in the relation for the inclination angle (30) and expanding for small values of the excess area Δ we obtain

$$\phi_0 = \frac{\pi}{4} - \frac{(9 + 23\lambda)\Delta^{1/2}}{16\sqrt{30\pi}}, \quad (32)$$

which agrees with the expression reported by Seifert¹³ for the no viscosity contrast case ($\lambda = 2$). The analogous result reported by Misbah¹⁴ contains a typo (140 should read 240). Our relation (32) is in good quantitative agreement with the experimental data of Kantsler and Steinberg⁷, as demonstrated on Figure 1. Eq. (31) implies that if $\Delta > 4h^2$, i.e. viscosity contrast higher than a critical value

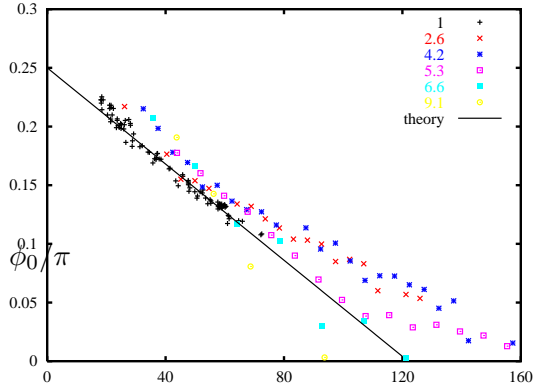
$$\lambda_c = -\frac{9}{23} + \frac{120}{23} \sqrt{\frac{2\pi}{15\Delta}} \quad (33)$$

no stationary tank-treading solution exists, as also pointed out by Misbah^{14,27}, and the vesicle starts to tumble.

B. Tumbling

The second fixed point of Eq. (26) corresponds to periodic vesicle deformation given by oscillating $j = 2$ modes around values

$$f'_{22} = h(\lambda), \quad f''_{22} = 0, \quad f'_{21} = 0, \quad f''_{21} = 0. \quad (34)$$



$$(9 + 23\lambda) \Delta^{-1/2}$$

FIG. 1: Stationary inclination angle in simple shear flow as function of the rescaled excess area for different viscosity contrasts. The symbols are experimental data from Kantsler and Steinberg⁸. The lines represent the linear small deformation theory (32).

If $f_{20}(0) \neq 0$, the $f_{20}(t)$ is also oscillating. All modes with $j \neq 2$ decay to zero and are not oscillating.

The time-periodic vesicle deformation depends strongly on the viscosity contrast as illustrated on Figure 2. Figure 2 (a) shows that close to the critical viscosity contrast the period of oscillations is long and the amplitude of oscillations of the f_{20} mode, which corresponds to out-of-the-flow-plane deformation, is significant. Experimentally the vesicle looks like trembling or “breathing”^{8,9}. The “breathing” motion has been discussed in parts by Misbah¹⁴ although the role of the f_{20} mode has not been made clear.

The mode oscillation frequency increases with viscosity contrast, as seen on Figure 2 (b). At high viscosity contrast it approaches the twice rate of rotation of the external flow, $\dot{\gamma}$. This can be seen from Eq. (26) where in the limit $\lambda \gg 1$ only the rotation terms survive. Since the f_{20} mode is not rotationally stabilized, its oscillation amplitude becomes negligible at high viscosity contrast; correspondingly the out-of-the-flow-plane deformation is suppressed. The periodic vesicle deformation corresponds to rigid body rotation, $f'_{22}(t) \sim \cos(t)$, $f''_{22}(t) \sim \sin(t)$.

In order to compare theory and experiment we first derive expressions for some experimentally measurable parameters. Experimentally only the deformation in the flow plane is observable. The vesicle contour represents an ellipse. Combining (14) and (30) we obtain

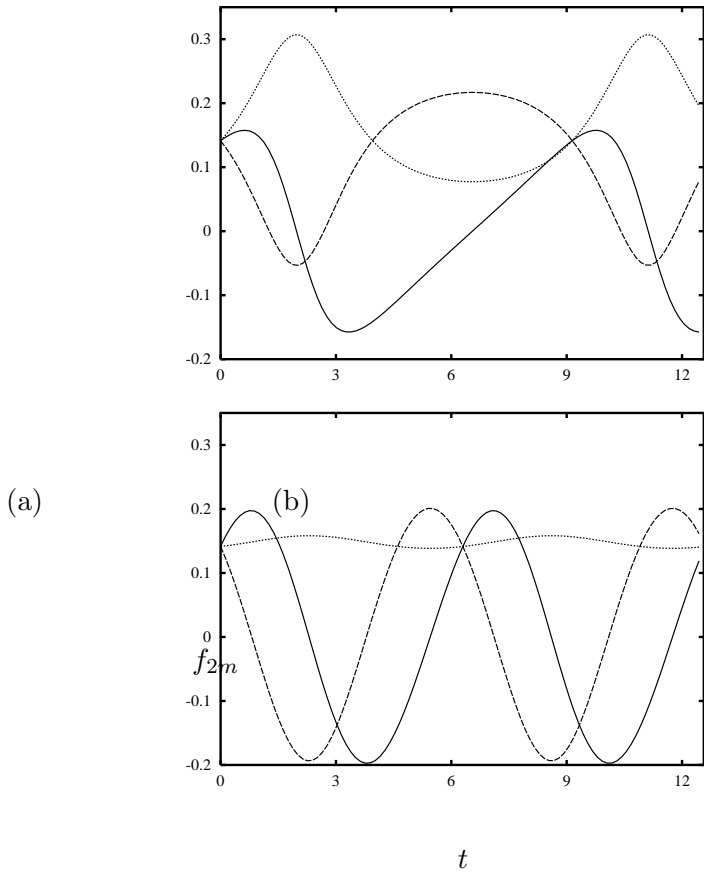


FIG. 2: Time dependence of the f_{2m} modes in the (a) breathing ($\lambda \gtrsim \lambda_c$) and (b) tumbling ($\lambda \gg \lambda_c$) regimes; solid, dashed and dotted lines represent the f_{22}'' , f_{22}' and f_{20} modes, respectively. The excess area is $\Delta = 0.2$. The viscosity contrasts are (a) $\lambda = 10$, (b) $\lambda = 100$. The initial conditions are $f_{22}'(0) = f_{22}''(0) = \sqrt{0.1\Delta}$; $f_{20}(0)$ is determined by the area constraint.

for the lengths of the major and minor axes

$$r_{max,min}(t) = 1 - f_{20}(t) \sqrt{\frac{5}{\pi}} \pm (\Delta - 2f_{20}^2(t))^{\frac{1}{2}} \sqrt{\frac{15}{2\pi}}, \quad (35)$$

where we have neglected the contributions from the $f_{2\pm 1}$ modes for the sake of simplicity. We see that the major and minor axes follow the oscillations of the f_{20} mode; the larger the f_{20} oscillation amplitude, the larger the amplitude in the r_{max} and r_{min} fluctuations. In the experiments of Kantsler and Steinberg⁸ the excess area $\bar{\Delta}$ corresponding to a prolate ellipsoidal shape with major and minor axes as seen in the flow plane was reported. Using the relation between the deformation in the flow plane and the excess area $(r_{max} - r_{min}) / (r_{max} + r_{min}) =$

$(15\bar{\Delta}/32\pi)^{\frac{1}{2}}$, reported first by Seifert¹³, we obtain

$$\bar{\Delta}(t) = \frac{\Delta - 2f_{20}^2(t)}{\left[1 - f_{20}(t)\sqrt{\frac{5}{16\pi}}\right]^2} \quad (36)$$

Unlike the true excess area Δ , which is constant, $\bar{\Delta}$ is time-dependent due to the fluctuations in the f_{20} mode, i.e. the out-of-the-flow-plane transfer of area.

The angle evolution is described by

$$\dot{\phi} = -\frac{1}{2} + \frac{h(\lambda)}{(\Delta - 2f_{20}^2(t))^{\frac{1}{2}}} \cos(2\phi(t)), \quad (37)$$

from which we infer that the tumbling period, defined as the time needed for a material point to return to its initial position, is given by

$$T_{tumble} = 4\pi \left[1 - \frac{4h(\lambda)^2}{\Delta}\right]^{-\frac{1}{2}}. \quad (38)$$

As already discussed, when the viscosity contrast is high the oscillations of the f_{20} mode are suppressed and $f_{20}(t) \approx f_{20}(0)$. In this case Eq. (37) becomes equivalent to the Keller–Skalak equation $\dot{\phi} = A + B \cos(2\phi)$, where the constants A and B are identified with $-1/2$ and $h(\lambda)/\sqrt{\Delta - 2f_{20}^2(0)}$, respectively.

We compared the time-dependent vesicle behavior with the experiments of Mader *et al.*⁹. A good agreement was obtained for the angle evolution, for example of their vesicle number 6 using reduced volume 0.988 instead of the reported 0.996. The difference is reasonable given the uncertainty with which the reduced volume is determined experimentally: it is computed assuming axial symmetry about the vesicle longest axis, which might not be always the case because of the presence of a non-zero f_{20} mode. Note that in the tank-treading regime, however, since the excess area is stored only in the $f_{2\pm 2}$ modes the vesicle is a prolate ellipsoid and the computation of the reduced volume is quite accurate. We also attempted to reproduce theoretically the experimental curves on Figure 4 of Kantsler and Steinberg⁸. The predicted tumbling frequency from Eq. (38) using viscosity contrast and excess area close the reported values was almost twice higher than the experimental data. One possible explanation is that our small-deformation theory fails for the large values of the excess area in this experiment ($\Delta \approx 1$).

C. Rheology

A suspension of vesicles can be described as a continuum with effective properties such as viscosity. The bulk stress of a dilute suspension with particle volume fraction ϕ is

$$\boldsymbol{\Sigma} = 2\mathbf{E} + \phi\mathbf{T}, \quad (39)$$

where \mathbf{T} is the stress associated with the vesicle disturbance velocity field. Rheological properties of interest are the shear viscosity, T_{xy} , and the normal stress differences, $N_1 = T_{xx} - T_{yy}$ and $N_2 = T_{yy} - T_{zz}$. Vesicle stress is directly related to the amplitudes of the velocity field $j = 2$ (20)²⁹

$$T_{xy} = -\frac{i}{8}\sqrt{\frac{6}{5\pi}}(\hat{c}_{220} - \hat{c}_{2-20}), \quad (40a)$$

$$N_1 = -\frac{1}{4}\sqrt{\frac{6}{5\pi}}(\hat{c}_{220} + \hat{c}_{2-20}), \quad (40b)$$

$$N_2 = -\frac{1}{2}N_1 + \frac{3}{4}\sqrt{\frac{1}{5\pi}}\hat{c}_{200}. \quad (40c)$$

where the relations between \hat{c} and c are given by (E6). Note that the c are the amplitudes of the disturbance velocity field outside the vesicle, $\mathbf{v}^{\text{out}} - \mathbf{v}^\infty$.

Stresses are obtained using the solution for the velocity field given in Appendix C. The vesicle contribution to the effective shear viscosity consists of contributions due to viscosity contrast and to membrane stresses

$$T_{xy} = \frac{5}{2}\frac{23\lambda-39}{23\lambda+9} + \chi^{-1}3i\sqrt{\frac{30}{\pi}}\frac{E(2,\sigma_0)(f_{22}-f_{2-2})}{23\lambda+9}. \quad (41)$$

where the shape deformation modes $f_{2\pm 2}$ are given by (C10). For a given excess area and viscosity contrast, viscosity is shear thinning, i.e. decreases with the increase in flow strength, and in the tank-treading regime it approaches a limiting value

$$T_{xy} = \frac{5}{2} - \Delta\frac{(23\lambda+9)}{16\pi}, \quad (42)$$

which is obtained by inserting the expression for the modes amplitude (C10) in (41) and taking into account (C12). Effective viscosity decreases from the value for a suspension of rigid spheres with the increase of the excess area because the deformable vesicles elongate

and thus offer less resistance to the flow. Increasing viscosity contrast also leads to decrease in the effective viscosity because vesicles align with the flow (the inclination angle (32) decreases).

Unlike the suspension of rigid spheres, a suspension of deformable vesicles exhibits normal stresses. In the tank-treading regime below the critical viscosity contrast, the magnitudes of the normal stresses are

$$N_1 = \frac{\Delta(23\lambda + 9)}{8\pi} \left[-1 + \frac{1920\pi}{\Delta(23\lambda + 9)^2} \right]^{\frac{1}{2}}, \quad (43a)$$

$$N_2 = -\frac{1}{2}N_1. \quad (43b)$$

D. Vesicle migration in the presence of wall

Knowledge of the normal stresses provides a quantitative insight into the phenomenon of vesicle lift-off from the wall in a wall-bounded shear flow. If the distance to the wall is much larger than the vesicle radius, the vesicle drift velocity normal to the rigid wall is proportional to the stress component in the direction of the plane unit normal³⁰, i.e. T_{yy} , $U_{\text{lift}} = -3/16h^2T_{yy}$. Combining Smart and Leighton's result³⁰ and our expression for $T_{yy} = -(N_1 - N_2)/3$ we obtain

$$U_{\text{lift}} = \frac{1}{16h^2} (N_1 - N_2). \quad (44)$$

Hence, the lift velocity far way from the wall can be estimated using the normal stresses expressions (43) and we obtain the relation

$$U_{\text{lift}} = \frac{c(\lambda, \Delta)}{h^2}, \quad (45)$$

where

$$c(\lambda, \Delta) = \frac{3}{32}N_1. \quad (46)$$

Similar type expressions have been reported in analytical studies^{22,31}, although the dependence on the excess area has not been presented in an explicit form. Eq. (46) shows that the more deformable the vesicle, i.e. the larger the excess area, the larger the migration velocity. Interestingly, at very small excess area we obtain from (43) that $N_1 \sim \Delta^{\frac{1}{2}}$ and vesicle

migration is independent of the viscosity contrast. The values of the prefactor (46) are of the same order of magnitude as reported in studies considering a tank-treading ellipsoid³¹ or numerical simulations of a vesicle with no viscosity contrast²⁰.

V. CONCLUSIONS AND OUTLOOK

This study explores the effect of viscosity contrast and membrane bending rigidity on vesicle behavior in simple shear flow and the rheology of a dilute suspension of vesicles. We developed a leading order small deformation theory to describe the dynamics of a vesicle in linear viscous flows. Expressions for the shape evolution equation, stress and velocity fields and the effective membrane tension, which is needed to enforce the area constraint, were derived using a formalism based on spherical harmonics. The main theoretical result of this study is contained in the shape evolution equation Eq. (24) and the expression for the effective tension Eq. (D5). The latter serves to eliminate the tension in favor of the excess area, which is the physically relevant parameter. The solution is applicable for any linear flow under transient or steady state conditions. In the case of simple shear flow, only the shape modes with the same spherical harmonic order as the external flow, $j = 2$, are perturbed; all other modes decay on a time scale set by the bending rigidity. Consequently, the shape evolution equations simplify to Eq. (26) and yields expressions for quantities that can be measured experimentally such as the inclination angle with respect to the flow direction, the lengths of the major and minor axes of the vesicle contour in the flow plane, etc. In the stationary tank-treading state, we show that in a simple shear flow the leading order deformation and stresses are independent of the membrane bending rigidity. Our theory is in quantitative agreement with experimental data for the vesicle deformation in the tank-treading and in the tumbling regimes. Non-Newtonian rheology with shear thinning viscosity and normal stresses is predicted for a suspension of vesicles. We also considered the vesicle dynamics in wall-bounded shear flow and presented a simple derivation of the leading order correction, in the distance to the wall, to the rate of vesicle migration away from the wall.

Several problems remain open. We discussed the main features of the time-dependent vesicle dynamics in linear flows, but this problem remains to be systematically explored. Although the quantitative agreement between predicted and experimentally observed⁹ be-

havior of tumbling vesicles with small excess area is encouragingly good, for vesicles with large excess area⁸ the agreement is poor, which might be due to the limitations of the leading order theory. Our analysis will be extended to consider higher-order perturbations, and hence elucidate the feedback from the flow on vesicle dynamics. Numerical simulations with a three-dimensional boundary integral method are being developed to explore the dynamics of highly non-spherical vesicle shapes. In wall-bounded flows, a more detailed description of the vesicle-wall hydrodynamic interactions is needed in order to predict the lift force quantitatively.

VI. ACKNOWLEDGMENTS

PV acknowledges the hospitality of the Theory Department at the Max-Planck Institute of Colloids and Interfaces, and in particular the group of Rumiana Dimova. This work has benefited from many fruitful discussions with Thomas Powers, Jerzy Blawdziewicz and Michael Loewenberg. The authors thank Reinhard Lipowsky, for his comments on the manuscript, and Manouk Abkarian, Vasiliy Kantsler and Victor Steinberg for providing their experimental data.

APPENDIX A: SPHERICAL HARMONICS

For the sake of completeness, we list the definitions of scalar and vector spherical harmonics^{32,33}. The normalized spherical scalar harmonics are defined as

$$Y_{jm}(\Omega) = \left[\frac{2j+1}{4\pi} \frac{(j-m)!}{(j+m)!} \right]^{1/2} (-1)^m P_j^m(\cos\theta) e^{im\varphi}, \quad (\text{A1})$$

where $\hat{\mathbf{r}} = \mathbf{r}/r$, (r, θ, φ) are the spherical coordinates, and $P_j^m(\cos\theta)$ are the Legendre polynomials. The vector spherical harmonics are defined as

$$\mathbf{y}_{jm0} = [j(j+1)]^{-1/2} r \nabla_{\Omega} Y_{jm}, \quad (\text{A2a})$$

$$\mathbf{y}_{jm1} = -i\hat{\mathbf{r}} \times \mathbf{y}_{jm0}, \quad (\text{A2b})$$

$$\mathbf{y}_{jm2} = \hat{\mathbf{r}} Y_{jm}, \quad (\text{A2c})$$

where ∇_{Ω} denotes the angular part of the gradient operator. \mathbf{y}_{jm0} and \mathbf{y}_{jm1} are tangential, while \mathbf{y}_{jm2} is normal to a sphere.

APPENDIX B: SHAPE EVOLUTION

The interface shape can be described by a function $F(\mathbf{r}, t)$, which represents interface as the set of points \mathbf{r} where $F(\mathbf{r}, t) \equiv 0$; it is given by the relation

$$F(\mathbf{r}, t) = r - r_s(\Omega, t) . \quad (\text{B1})$$

where r_s is the position of the surface in a coordinate system centered in the vesicle. The evolution of the interface is described by³⁴

$$\frac{\partial F}{\partial t} + \mathbf{v}_s \cdot \nabla F = 0 , \quad (\text{B2})$$

where \mathbf{v}_s is the fluid velocity at the vesicle interface. The outward normal vector is defined as

$$\mathbf{n} = \frac{\nabla F}{|\nabla F|} . \quad (\text{B3})$$

The mean and Gaussian curvatures are calculated using the normal vector

$$H = \frac{1}{2} \nabla \cdot \mathbf{n} , \quad (\text{B4})$$

$$K = \frac{1}{2} \nabla \cdot (\mathbf{n} \nabla \cdot \mathbf{n} + \mathbf{n} \times \nabla \times \mathbf{n}) . \quad (\text{B5})$$

For small deviations from sphericity²⁵

$$\mathbf{n}(\Omega) = \hat{\mathbf{r}} - f_{jm} [j(j+1)]^{\frac{1}{2}} \mathbf{y}_{jm0} , \quad (\text{B6})$$

$$H(\Omega) = 1 + \frac{1}{2} (j+2)(j-1) f_{jm} Y_{jm} . \quad (\text{B7})$$

Expanding around sphere, for the linear flow (2), at leading order $O(\lambda^{-1}\varepsilon)$ Eq. (B2) yields

$$\frac{\partial f_{jm}}{\partial t} = c_{jm2} + \omega \frac{im}{2} f_{jm} \quad \text{at } r = 1 . \quad (\text{B8})$$

The second term represents the rotation of the deformed shape.

APPENDIX C: LEADING ORDER PERTURBATION SOLUTION

At leading order, in the membrane interfacial stresses (6) the terms H^3 and HK cancel and only $\nabla_s^2 H$ remains

$$\nabla_s^2 H = -\frac{1}{2}j(j+1)(j-1)(j+2)f_{jm}Y_{jm}. \quad (\text{C1})$$

The first term in Eq. (6) yields

$$\sigma H = \left(\frac{1}{2}\sigma_0(j-1)(j+2)f_{jm} + \sigma_{jm}\right)Y_{jm}. \quad (\text{C2})$$

The isotropic (Laplace) part of the stress, σ_0 , has no importance in dynamics, and $\sigma_{jm}f_{jm}$ is a higher order term, therefore these are omitted. On a sphere $\nabla_s\sigma$ becomes simply $\sqrt{j(j+1)}\sigma_{jm}\mathbf{y}_{jm0}$ according to Eq. (A2a).

All modes that contribute to the excess area are affected by the flow. Therefore, we will present results for any j . In this way, the theory can be applied to fluctuating vesicles and other types of flow, e.g. quadratic (Poiseuille) flow.

The incompressibility condition (8) implies that the amplitudes of the velocity disturbance field (20) are related

$$c_{jm2} = \frac{1}{2}\sqrt{j(j+1)}c_{jm0}. \quad (\text{C3})$$

At leading order the stress balance reads

$$\hat{\mathbf{r}} \cdot \mathbf{T}^{\text{out}} - (\lambda - 1)\hat{\mathbf{r}} \cdot \mathbf{T}^{\text{in}} = \mathbf{t}^{\text{mem}}. \quad (\text{C4})$$

It gives a relation for the tractions (F3), which is linear in j and m

$$\boldsymbol{\tau}_{jmq}^{\text{out}} - (\lambda - 1)\boldsymbol{\tau}_{jmq}^{\text{in}} = \mathbf{t}_{jmq}^{\text{mem}}. \quad (\text{C5})$$

The tangential interfacial stress has an ‘‘irrotational’’ component

$$\mathbf{t}_{jm0}^{\text{mem}} = -\chi^{-1}\sqrt{j(j+1)}\sigma_{jm}. \quad (\text{C6})$$

The normal component of the membrane stress is

$$\mathbf{t}_{jm2}^{\text{mem}} = \chi^{-1}(2\sigma_{jm} + E(j, \sigma_0)f_{jm}). \quad (\text{C7})$$

The tangential balance (C6) determines the tension distribution in terms of the shape parameters

$$\begin{aligned} \sigma_{jm} = & -\chi c_{jm0}^{\infty} \frac{2(1+2j)}{\sqrt{j(j+1)}} + \chi c_{jm2}^{\infty} \frac{3(2j+1)}{j(j+1)} \\ & + \chi c_{jm0}^{\infty} \frac{(3+\lambda(j-1))}{2\sqrt{j(j+1)}}. \end{aligned} \quad (\text{C8})$$

Finally, the normal stress balance (C7) yields c_{jm0} . Substituting c_{jm2} in Eq. (B8) yields for the coefficients in the evolution equation (24)

$$\begin{aligned} C(\lambda, j, m) = & d(\lambda, j)^{-1} \left[c_{jm0}^{\infty} \sqrt{j(j+1)} (2j+1) \right. \\ & \left. + c_{jm2}^{\infty} (4j^3 + 6j^2 - 4j - 3) \right] \end{aligned} \quad (\text{C9a})$$

and

$$\Gamma(\lambda, \sigma_0, j) = -E(j, \sigma_0) \frac{j(j+1)}{d(\lambda, j)} \quad (\text{C9b})$$

where

$$d(\lambda, j) = 9\lambda^{-1} + (-5 + 3j^2 + 2j^3) \quad (\text{C9c})$$

and

$$E(j, \sigma) = (j+2)(j-1)(j(j+1) + \sigma). \quad (\text{C9d})$$

For a simple shear flow (25), solving Eq.(24) for the stationary amplitudes in the tank-treading regime gives

$$f_{2\pm 2} = \mp \frac{i\chi 10 \sqrt{\frac{2\pi}{15}}}{E(2, \sigma_0) \mp i\chi \frac{(9+23\lambda)}{6}} \quad (\text{C10})$$

and for the inclination angle

$$\phi_0 = \frac{1}{2} \arctan \left[\frac{6E(2, \sigma_0)}{\chi(9+23\lambda)} \right]. \quad (\text{C11})$$

These expressions agree with Seifert's results for a vesicle with no viscosity contrast ($\lambda = 2$)¹³. At long times, the excess area is stored in the $f_{2\pm 2}$ modes only. Substituting the tension (D5) in (C9d) leads to

$$E(2, \sigma_0) = \chi(23\lambda + 9) \sqrt{-1 + \frac{1920\pi}{(23\lambda + 9)^2 \Delta}}. \quad (\text{C12})$$

Thus the dependence of the mode amplitudes on the capillary number in Eq.(C10) cancels. Expanding Eq. (C11) for small values of the excess area Δ we obtain (32).

Note that the surface solenoidal velocity field \mathbf{u}_{jm1}^\pm satisfies identically the incompressibility condition (8) and a stress boundary condition

$$\tau_{jm1}^{\text{out}} - (\lambda - 1) \tau_{jm1}^{\text{in}} = 0 \quad (\text{C13})$$

which corresponds to a spherical drop with clean surface. Thus, the surface solenoidal component of the velocity field is not disturbed by the vesicle at this order and $c_{jm1} = c_{jm1}^\infty$.

For the sake of completeness we mention the relation between our notation and the one used by Seifert¹³

$$\begin{aligned} c_{jm2} &= X_{jm} , \\ c_{jm0} &= (Y_{jm} + 2X_{jm}) [j(j+1)]^{-\frac{1}{2}} . \end{aligned} \quad (\text{C14})$$

APPENDIX D: AREA CONSTRAINT AND THE TENSION

The area constraint (22) serves to determine the isotropic part of the tension σ_0 . We can split Eq. (C9b) into

$$\Gamma(\lambda, \sigma_0, j) = \alpha(\lambda, j) + \sigma_0 \beta(\lambda, j) , \quad (\text{D1})$$

where

$$\alpha(\lambda, j) = -2a(j) \frac{[j(j+1)]^2}{d(\lambda, j)} , \quad (\text{D2})$$

and

$$\beta(\lambda, j) = -2a(j) \frac{j(j+1)}{d(\lambda, j)} . \quad (\text{D3})$$

The modes have to satisfy the area constraint $\dot{\Delta} = 0$, i.e.

$$\sum_{jm} a_j \dot{f}_{jm} f_{jm}^* = 0 \quad (\text{D4})$$

Multiplying the evolution equations (24) by $a(j) f_{jm}^*$, summing up and solving for the tension leads to

$$\sigma_0 = - \frac{\sum_{jm} a(j) [C(\lambda, j, m) f_{jm}^* + \chi^{-1} \alpha(\lambda, j) f_{jm} f_{jm}^*]}{\chi^{-1} \sum_{jm} a(j) \beta(\lambda, j) f_{jm} f_{jm}^*} . \quad (\text{D5})$$

The complicated dependence of the tension on the shape modes makes the evolution equations Eq. (24) nonlinear.

APPENDIX E: FUNDAMENTAL SET OF VELOCITY FIELDS

Following the definitions given in Blawdziewicz *et al.*²⁹, we list the expressions for the functions $\mathbf{u}_{jmq}^\pm(r, \Omega)$

$$\begin{aligned} \mathbf{u}_{jm0}^- &= \frac{1}{2}r^{-j}(2-j+jr^{-2})\mathbf{y}_{jm0} \\ &+ \frac{1}{2}r^{-j}[j(j+1)]^{1/2}(1-r^{-2})\mathbf{y}_{jm2}, \end{aligned} \quad (\text{E1a})$$

$$\mathbf{u}_{jm1}^- = r^{-j-1}\mathbf{y}_{jm1}, \quad (\text{E1b})$$

$$\begin{aligned} \mathbf{u}_{jm2}^- &= \frac{1}{2}r^{-j}(2-j)\left(\frac{j}{1+j}\right)^{1/2}(1-r^{-2})\mathbf{y}_{jm0} \\ &+ \frac{1}{2}r^{-j}(j+(2-j)r^{-2})\mathbf{y}_{jm2}. \end{aligned} \quad (\text{E1c})$$

$$\begin{aligned} \mathbf{u}_{jm0}^+ &= \frac{1}{2}r^{j-1}(-(j+1)+(j+3)r^2)\mathbf{y}_{jm0} \\ &- \frac{1}{2}r^{j-1}[j(j+1)]^{1/2}(1-r^2)\mathbf{y}_{jm2}, \end{aligned} \quad (\text{E2a})$$

$$\mathbf{u}_{jm1}^+ = r^j\mathbf{y}_{jm1}, \quad (\text{E2b})$$

$$\begin{aligned} \mathbf{u}_{jm2}^+ &= \frac{1}{2}r^{j-1}(3+j)\left(\frac{j+1}{j}\right)^{1/2}(1-r^2)\mathbf{y}_{jm0} \\ &+ \frac{1}{2}r^{j-1}(j+3-(j+1)r^2)\mathbf{y}_{jm2}. \end{aligned} \quad (\text{E2c})$$

On a sphere $r = 1$ these velocity fields reduce to

$$\mathbf{u}_{jmq}^\pm = \mathbf{y}_{jmq}. \quad (\text{E3})$$

Hence, \mathbf{u}_{jm0}^\pm and \mathbf{u}_{jm1}^\pm are tangential, and \mathbf{u}_{jm2}^\pm is normal to a sphere. In general, a vector velocity field which is tangential to a surface with normal \mathbf{n} has an irrotational component²³

$$\mathbf{n} \cdot (\nabla_s \times \mathbf{v}^{irr}) = 0, \quad (\text{E4})$$

and solenoidal component

$$\nabla_s \cdot \mathbf{v}^{sol} = 0. \quad (\text{E5})$$

On a sphere, the irrotational component is identified with the $q = 0$ vector spherical harmonic, and the solenoidal corresponds to the $q = 1$ vector spherical harmonic.

Next we list the relation between our velocity basis and the one needed for the stresses calculation (40)

$$\hat{c}_{jm0} = \frac{(2j+1)(2j-1)[j(j+1)]^{1/2}}{j+1}c_{jm0} + \frac{j(2j+1)(2j-1)}{j+1}c_{jm2}. \quad (\text{E6})$$

The complete expressions can be found in Blawdziewicz et al.²⁹.

APPENDIX F: HYDRODYNAMICS STRESSES

The bulk hydrodynamics stresses, normalized by viscosity ratio, are

$$\mathbf{T} = -p\mathbf{I} + \nabla'\mathbf{u}. \quad (\text{F1})$$

where ∇' denotes the symmetric, traceless gradient operator

$$\nabla'\mathbf{u} = \frac{1}{2}[\nabla\mathbf{u} + (\nabla\mathbf{u})^T] - \frac{1}{3}\nabla \cdot \mathbf{u} \quad (\text{F2})$$

The hydrodynamic tractions exerted on a surface with a normal vector \mathbf{n} are $\mathbf{n} \cdot \mathbf{T}$

$$\boldsymbol{\tau} \equiv \mathbf{n} \cdot \mathbf{T} = \tau_{jmq}\mathbf{Y}_{jmq} \quad (\text{F3})$$

In the particular case of a sphere characterized with a normal vector $\hat{\mathbf{r}}$, the viscous tractions are linearly related to the velocity field

$$\tau_{jmq}^{\text{out}} = \sum_{q'}^2 c_{jm q'}^{\infty} (\Theta_{q'q}^+ - \Theta_{q'q}^-) + \sum_{q'}^2 c_{jm q'} \Theta_{q'q}^- \quad (\text{F4a})$$

$$\tau_{jmq}^{\text{in}} = \sum_{q'}^2 c_{jm q'} \Theta_{q'q}^+ \quad (\text{F4b})$$

where $\Theta_{q'q}^{\pm}$ are obtained from the velocity fields (E1)–(E2)²⁹,

$$\Theta_{q'q}^+(j) = \begin{pmatrix} 2j+1 & 0 & -3\left(\frac{j+1}{j}\right)^{\frac{1}{2}} \\ 0 & j-1 & 0 \\ -3\left(\frac{j+1}{j}\right)^{\frac{1}{2}} & 0 & 2j+1+\frac{3}{j} \end{pmatrix} \quad (\text{F5})$$

$$\Theta_{qq'}^-(j) = \begin{pmatrix} -2j-1 & 0 & 3\left(\frac{j}{j+1}\right)^{\frac{1}{2}} \\ 0 & -j-2 & 0 \\ 3\left(\frac{j}{j+1}\right)^{\frac{1}{2}} & 0 & -2j-1-\frac{3}{j+1} \end{pmatrix} \quad (\text{F6})$$

In the derivation of the above expressions we have used that

$$\hat{\mathbf{r}} \cdot \nabla' \mathbf{v} = r \frac{d}{dr} \left(\frac{\mathbf{v}}{r} \right) + \frac{1}{r} \nabla (\mathbf{v} \cdot \mathbf{r}) . \quad (\text{F7})$$

- * Present address: Thayer School of Engineering, Dartmouth College, Hanover, NH 03755.; Electronic address: petia.vlahovska@dartmouth.edu
- ¹ J. M. Rallison, *Ann. Rev. Fluid Mech.* **16**, 45 (1984).
- ² H. A. Stone, *Ann. Rev. Fluid Mech.* **26**, 65 (1994).
- ³ D. Barthes-Biesel, *Physica A* **172**, 103 (1991).
- ⁴ P. L. Luisi and P. Walde, *Giant vesicles* (Wiley, New York, 2000).
- ⁵ U. Seifert, *Advances in physics* **46**, 13 (1997).
- ⁶ K. H. de Haas, C. Blom, D. van den Ende, M. H. G. Duits, and J. Mellema, *Phys. Rev. E* **56**, 7132 (1997).
- ⁷ V. Kantsler and V. Steinberg, *Phys. Rev. Lett.* **95**, 258101 (2005).
- ⁸ V. Kantsler and V. Steinberg, *Phys. Rev. Lett.* **96**, 036001 (2006).
- ⁹ M.-A. Mader, V. Vitkova, M. Abkarian, A. Viallat, and T. Podgorski, *Eur. Phys. J. E* **19**, 389 (2006).
- ¹⁰ M. Kraus, W. Wintz, U. Seifert, and R. Lipowsky, *Phys.Rev.Lett.* **77**, 3685 (1996).
- ¹¹ J. Beaucourt, F. Rioual, T. Seon, T. Biben, and C. Misbah, *Phys. Rev. E* **69**, 011906 (2004).
- ¹² H. Noguchi and G. Gompper, *Phys. Rev. Lett.* **93**, 258102 (2004).
- ¹³ U. Seifert, *Eur. Phys. J. B* **8**, 405 (1999).
- ¹⁴ C. Misbah, *Phys. Rev. Lett.* **96**, 028104 (2006).
- ¹⁵ P. Olla, *Physica A* **278**, 87 (2000).
- ¹⁶ S. R. Keller and R. Skalak, *J. Fluid Mech.* **120**, 27 (1982).
- ¹⁷ M. Abkarian and A. Viallat, *Biophys. J.* **89**, 1055 (2005).
- ¹⁸ B. Lorz, R. Simson, J. Nardi, and E. Sakmann, *Europhys. Lett.* **51**, 468 (2000).

- ¹⁹ M. Abkarian, C. Lartigue, and A. Viallat, Phys. Rev. Lett. **88**, 068103 (2002).
- ²⁰ S. Sukumaran and U. Seifert, Phys. Rev. E **64**, 011916 (2001).
- ²¹ I. Cantat and C. Misbah, Phys. Rev. Lett. **83**, 235 (1999).
- ²² U. Seifert, Phys. Rev. Lett. **83**, 876 (1999).
- ²³ J. Bławdziewicz, E. Wajnryb, and M. Loewenberg, J. Fluid Mech. **395**, 29 (1999).
- ²⁴ B. Cichocki, B. U. Felderhof, and R. Schmitz, PhysicoChem. Hyd. **10**, 383 (1988).
- ²⁵ P. Vlahovska, J. Bławdziewicz, and M. Loewenberg, Phys. Fluids **17**, Art. No.103103 (2005).
- ²⁶ P. Vlahovska, Ph.D. thesis, Yale University (2003), pdf file available by email: petia@aya.yale.edu.
- ²⁷ T. Biben and C. Misbah, Phys. Rev. E **67**, 031908 (2003).
- ²⁸ D. Barthes-Biesel and H. Sgaier, J. Fluid. Mech. **160**, 119 (1985).
- ²⁹ J. Bławdziewicz, P. Vlahovska, and M. Loewenberg, Physica A **276**, 50 (2000).
- ³⁰ J. R. Smart and D. T. Leighton, Phys. Fluids A **3**, 21 (1990).
- ³¹ P. Olla, J.Phys. II France **7**, 1533 (1997).
- ³² M. N. Jones, *Spherical Harmonics and Tensors for Classical Field Theory* (Wiley, New York, 1985).
- ³³ D. A. Varshalovich, A. N. Moskalev, and V. K. Kheronskii, *Quantum Theory of Angular Momentum* (World Scientific, Singapore, 1988).
- ³⁴ L. G. Leal, *Laminar Flow and Convective Transport Processes* (Butterworth-Heinemann, Boston, 1992).